



**HAL**  
open science

# Controllability and control synthesis of underactuated magnetic microrobots

Matthieu Fruchard

► **To cite this version:**

Matthieu Fruchard. Controllability and control synthesis of underactuated magnetic microrobots. *Automatica*, 2023, 149, pp.110823. 10.1016/j.automatica.2022.110823 . hal-04093806

**HAL Id: hal-04093806**

**<https://hal.science/hal-04093806>**

Submitted on 10 May 2023

**HAL** is a multi-disciplinary open access archive for the deposit and dissemination of scientific research documents, whether they are published or not. The documents may come from teaching and research institutions in France or abroad, or from public or private research centers.

L'archive ouverte pluridisciplinaire **HAL**, est destinée au dépôt et à la diffusion de documents scientifiques de niveau recherche, publiés ou non, émanant des établissements d'enseignement et de recherche français ou étrangers, des laboratoires publics ou privés.

# Controllability and Control Synthesis of Underactuated Magnetic Microrobots

Matthieu Fruchard <sup>a,1</sup>

<sup>a</sup> *University of Orléans, Insa CVL, PRISME, EA 4229, Orléans, France*

---

## Abstract

The control of multiple magnetic microrobots is of particular interest for therapeutic applications. Yet the controllability of such a system is not straightforward since, on most of such systems designs, there is only a single control input per axis. The paper addresses the controllability and control synthesis for several magnetic microrobots navigating in blood vessels. First, controllability requires the microrobots to magnetically interact in order to achieve trajectory tracking along an admissible reference trajectory, whether swimming at low or high Reynolds. Then the resulting nonlinear system is shown to be diffeomorphic to different nonlinear canonical forms depending on the choice of the microrobots, so that the stabilization of the system along any admissible reference trajectory can be achieved using a backstepping controller synthesis, yet sometimes at the price of a zero dynamics stability analysis. Simulation results illustrate the efficiency of the proposed approach.

*Key words:* controllability; underactuated multi-agent system; nonlinear control synthesis; medical microrobotics.

---

## 1 Introduction

The control of untethered microrobots using the vascular network is receiving a growing interest since they can perform minimally invasive and targeted surgery or diagnosis, whilst accessing to remote places with lessened side effects. Deported magnetic actuation is appealing since it avoids an embedded energy source, resulting in an improved miniaturization and payload ratio. Different propulsion designs have been studied: elastic flagellated Lagomarsino et al. (2003); Evans and Lauga (2010), helical tailed Dreyfus et al. (2005); Zhang et al. (2010), or bead pulled robots Abbott et al. (2009); Mathieu et al. (2006). This emerging field has at first mainly focused on feasibility Nelson et al. (2010), then on controllability Giraldi and Pomet (2017) and control and observation Fruchard et al. (2014) issues for a single robot. However some applications, such as drug targeting or brachytherapy, require that enough payload is released in the vicinity of a tumor. On the other hand, avoiding arterial embolization hazards induces limitations on the microrobot size, and so on the available payload, hence the interest in controlling multiple robots.

Literature abounds with micro multi-agent strategies,

---

*Email address:* [matthieu.fruchard@univ-orleans.fr](mailto:matthieu.fruchard@univ-orleans.fr) (Matthieu Fruchard).

<sup>1</sup> Corresponding author.

yet there is an obstruction in the present case: the microrobots are often controlled using a single control input, either using electrostatic setups Donald et al. (2008), electromagnetic setups Floyd et al. (2009); Frutiger et al. (2010); Servant et al. (2015), or Magnetic Resonance Imaging (MRI) devices Martel and Mohammadi (2010) actuators. Consequently, multiple magnetic robots modeling results in a nonlinear underactuated system. Vartholomeos et al. (2012) parameterized the input as a sequence of pulses with different widths that exploited the induced motion difference to control independently different robots. However, this work aimed at a position open-loop control and therefore suffered from a lack of robustness. Floyd et al. (2011); Diller et al. (2012) proposed to exploit the natural frequency differences between some robots to actuate one or part of the considered magnetic microrobots with a point to point control objective. In Salehizadeh and Diller (2017) the authors took advantage of a rotating magnetic field to control the distance and orientation of two agents operating in close vicinity through the modulation of their attractive-repulsive interaction. Eqtami et al. (2014) addressed more formally the control of two microrobots using model predictive control to perform a fixed point stabilization. To exhibit a solution, they assumed the existence of a solution to the initial optimal control objective, *i.e.* that the system is locally controllable from the initial point, but did not focus on controllability issues. The controllability of two non inertial micro-

robots has already been studied in Salehizadeh and Diller (2017, 2021), yet only considering their relative position controllability; a full state controllability analysis has been provided in Fruchard et al. (2020) using the linear test, yet only a sufficient condition is given.

The present paper addresses the control of magnetic interacting microrobots facing the pulsatile blood flow in order to stabilize their full state along a reference trajectory, using the same single control input. The paper contribution is twofold: *i*) conditions under which these systems are controllable are investigated, which is –to our knowledge– the first full state commandability result for such an underactuated multi-agent microrobotic system, and *ii*) Lyapunov stabilizing control laws are synthesized exploiting transformations to nonlinear canonical forms, depending on the system design and parameters. Finally, simulations results illustrate the stability of the proposed controller, for an inertial 2-microrobot system and for a non inertial 5-microrobot system.

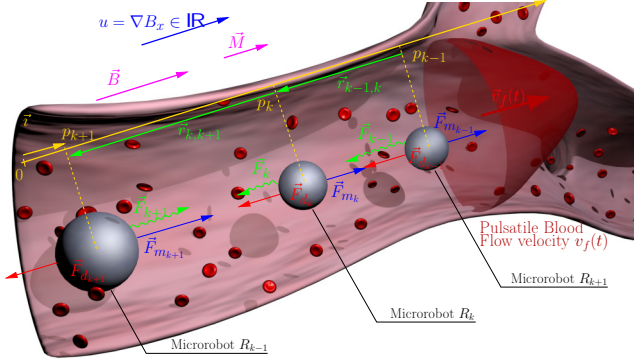


Fig. 1. Forces exerting on a magnetic microrobot ( $R_k$ ) and its closest neighbours ( $R_{k-1}$ ), ( $R_{k+1}$ ): the drag force  $\vec{F}_{d,k}$ , the magnetic motive force  $\vec{F}_{m,k}$ , and  $\vec{F}_k$  the net magnetic force interaction acting on robot ( $R_k$ ). A single control input  $u = \nabla B_x \in \mathbb{R}$  is used to control all the microrobots in a frame  $\mathcal{F}(0, \vec{i})$ .

## 2 Modeling

Spherical microrobots ( $R_k$ ) navigating in a blood vessel are localized by their positions  $p_k$  in the frame  $\mathcal{F}(0, \vec{i})$ , see Figure 1. Each microrobot is affected by the drag force, the motive magnetic force and the magnetic interaction between the robots, detailed hereinafter. The magnetic field is supposed stationary, like in MRI devices.

### 2.1 Forces

In the blood, a moving spherical microrobot ( $R_k$ ) of radius  $r_k$  experiences a drag force that opposes its motion. Even if the proposed approach can be extended *mutatis mutandis* to nonlinear drag force or to non-Newtonian blood modeling, as *e.g.* in Arcese et al. (2012, 2013), it

is here assumed –for sake of simplicity– that the drag force is linear:

$$\vec{F}_{d,k} = -m_k d_k (\dot{p}_k - v_f(t)) \vec{i}, \quad d_k = \frac{9\eta}{2\beta_k \rho_k r_k^2} \quad (1)$$

where  $\beta_k$  is a dimensionless ratio related to the partial vessel occlusion by the robot Haberman and Sayre (1958), and  $\dot{p}_k - v_f(t)$  denotes the relative velocity between the robot ( $R_k$ ) and the fluid.  $\eta$ ,  $\rho_k$  and  $m_k$  denote respectively the blood viscosity, the microrobot ( $R_k$ ) density and mass.

A robot of magnetization  $\vec{M}_k$  and ferromagnetic ratio  $\tau_{m,k}$  exposed to a magnetic field gradient input  $u = \nabla B_x$  is pulled by a magnetic force Arcese et al. (2012):

$$\vec{F}_{m,k} = m_k a_k u \vec{i}, \quad a_k = \tau_{m,k} M_k / \rho_k. \quad (2)$$

Let  $\mu_0$  and  $\vec{M}_k = \frac{4}{3}\pi\tau_{m,k}r_k^3\vec{M}_k$  denote the vacuum permeability and the ( $R_k$ ) microrobot magnetic moment, and  $\vec{r}_{k,i} = (p_i - p_k)\vec{i}$ . The magnetic interaction force  $\vec{F}_k$  exerted by other microrobots on ( $R_k$ ) is given by Vartholomeos and Mavroidis (2012). Since  $\vec{B} = B_0\vec{i}$ , and since this force is short ranged, we consider only a two-closest neighbours interaction, so:

$$\vec{F}_k = m_k \left( \frac{j_{k-1}}{\|\vec{r}_{k-1,k}\|^4} - \frac{i_k}{\|\vec{r}_{k,k+1}\|^4} \right) \vec{i} \quad (3)$$

$$i_k = \frac{3\mu_0 \mathcal{M}_k \mathcal{M}_{k+1}}{2\pi m_k} \frac{\vec{r}_{k+1,k} \cdot \vec{i}}{\|\vec{r}_{k,k+1}\|}, \quad j_k = \frac{i_k m_k}{m_{k+1}}, \quad i_k j_k \geq 0.$$

### 2.2 Two Inertial Microrobots

Let  $x^T = (p_1 \ p_2 \ \dot{p}_1 \ \dot{p}_2) \in \mathcal{X}$  denote the state vector where  $\mathcal{X}$  is any connected subset of either  $\mathcal{X}^+ = \{x \in \mathbb{R}^4 : x_1 - x_2 > 0\}$  or  $\mathcal{X}^- = \{x \in \mathbb{R}^4 : x_1 - x_2 < 0\}$  depending on the relative initial positions  $x_1$  and  $x_2$ . Applying the Newton's second law using (1), (2) and (3) yields:

$$(\mathcal{S}_x) \begin{cases} \dot{x}_1 = x_3 \\ \dot{x}_2 = x_4 \\ \dot{x}_3 = -d_1(x_3 - v_f) - \frac{i_1}{(x_1 - x_2)^4} + a_1 u \\ \dot{x}_4 = -d_2(x_4 - v_f) + \frac{j_1}{(x_1 - x_2)^4} + a_2 u \end{cases} \quad (4)$$

Along any  $\mathcal{C}^1$  admissible reference trajectory  $(x_r, u_r)$  with  $x_r^T(t) = (x_{1r} \ x_{2r} \ \dot{x}_{1r} \ \dot{x}_{2r}) (t)$  satisfying (4), there exists a  $\mathcal{C}^2$  distance function  $d_{1,2}(t) \in \mathcal{D} \subset \mathbb{R} \setminus \{0\}$ :  $d_{1,2}(t) = x_{1r}(t) - x_{2r}(t)$ . Let  $\tilde{x} = x - x_r$  denote an error state, the resulting error dynamics is an affine nonlinear

control system with drift:

$$\begin{cases} \dot{\tilde{x}} = f(\tilde{x}) + g\tilde{u} \\ f(\tilde{x}) = \begin{pmatrix} \tilde{x}_3 \\ \tilde{x}_4 \\ -d_1\tilde{x}_3 - i_1\delta_1(\tilde{x}) \\ -d_2\tilde{x}_4 + j_1\delta_1(\tilde{x}) \end{pmatrix}, g = \begin{pmatrix} 0 \\ 0 \\ a_1 \\ a_2 \end{pmatrix} \end{cases} \quad (5a)$$

with  $\tilde{u} = u - u_r(t)$ ,  $\tilde{\mathcal{X}}$  a connected subset of either  $\tilde{\mathcal{X}}^+ = \{\tilde{x} \in \mathbb{R}^4 : \tilde{x}_1 - \tilde{x}_2 + d_{1,2}(t) > 0\}$  or  $\tilde{\mathcal{X}}^- = \{\tilde{x} \in \mathbb{R}^4 : \tilde{x}_1 - \tilde{x}_2 + d_{1,2}(t) < 0\}$ , and the nonlinear function:

$$\delta_1 : \tilde{x} \mapsto \frac{1}{(\tilde{x}_1 - \tilde{x}_2 + d_{1,2}(t))^4} - \frac{1}{d_{1,2}^4(t)}. \quad (6)$$

### 2.3 A Finite Number $m$ of Non Inertial Microrobots

In a Stokes flow,  $Re \ll 1$  so inertial effects can be neglected Purcell (1977); Tikhonov (1952). Rewriting (5) for  $m$  non inertial microrobots leads to the following error system:

$$\begin{cases} \dot{\tilde{x}} = f(\tilde{x}) + g\tilde{u} \\ f(\tilde{x}) = \begin{pmatrix} -\epsilon_1\delta_1 \\ \vdots \\ \epsilon_{k-1}\delta_{k-1} - \epsilon_k\delta_k \\ \vdots \\ \epsilon_{m-1}\delta_{m-1} \end{pmatrix}, g = \begin{pmatrix} \alpha_1 \\ \vdots \\ \alpha_k \\ \vdots \\ \alpha_m \end{pmatrix} \end{cases} \quad (7a)$$

where  $\tilde{x} = (p_1 - x_{1r} \dots p_k - x_{kr} \dots p_m - x_{mr})^T \in \tilde{\mathcal{X}}_m \subset \mathbb{R}^m$  is the state vector composed of the position errors of the  $m$  robots ( $R_k$ ), and:

$$\delta_k : \tilde{x} \mapsto \frac{1}{(\tilde{x}_k - \tilde{x}_{k+1} + d_{k,k+1}(t))^4} - \frac{1}{d_{k,k+1}^4(t)} \quad (8)$$

with  $d_{k,k+1}(t)$  the ( $R_k$ ) to ( $R_{k+1}$ ) reference distance,  $\epsilon_k = \frac{i_k}{d_k}$ ,  $\epsilon_k = \frac{j_k}{d_{k+1}}$  so that  $\epsilon_k \epsilon_k \geq 0$  and  $\alpha_k = \frac{a_k}{d_k}$ . System  $\mathcal{S}_m^{ni}$  is defined on any connected subset  $\tilde{\mathcal{X}}_m$  of  $\tilde{\mathcal{X}}_m^- = \{\tilde{x} \in \mathbb{R}^m : \tilde{x}_1 < \tilde{x}_2 - d_{1,2} < \dots < \tilde{x}_m - \sum_{i=1}^{m-1} d_{i,i+1}\}$  or  $\tilde{\mathcal{X}}_m^+ = \{\tilde{x} \in \mathbb{R}^m : \tilde{x}_1 > \tilde{x}_2 - d_{1,2} > \dots > \tilde{x}_m - \sum_{i=1}^{m-1} d_{i,i+1}\}$ . Since the magnetic interaction is a short range force, one considers that microrobot ( $R_k$ ) interacts only with its two closest neighbours ( $R_{k-1}$ ) and ( $R_{k+1}$ ).

## 3 Problem statement

In system  $\mathcal{S}_x$ , the positions  $p = (p_1 \ p_2)$  and velocities  $v = (\dot{p}_1 \ \dot{p}_2)$  belong to a  $2D$  space, whereas the control input  $u$  is scalar; underactuation degree is even higher for system  $\mathcal{S}_m^{ni}$ . Thence we face an underactuated microrobotic system with drift whose full state controllability has not yet been addressed in the literature, even though partial controllability has been addressed in Salehizadeh and Diller (2017, 2021).

Another consequence of the underactuation is that all reference trajectories are not feasible by the microrobotic system. Admissible reference trajectories thus have to be defined to solve the trajectory planning issue, *e. g.* using differential flatness whenever the system is flat or the procedure detailed in Fruchard et al. (2020). Finally, how to synthesize a control law that stabilizes the state  $\tilde{x}$  along any admissible reference trajectory? One can rely either on linear or on nonlinear approaches. Yet, even with a single microrobot, works based on linear controllers, *e.g.* Tamaz et al. (2008); Mehrtash and Khamesee (2011); Choi et al. (2010), report instabilities and important oscillations for PID or LQR controllers can not deal properly with nonlinear perturbed systems. Besides, in the case of a multi-agent system, the nonlinear terms  $\delta_k(\tilde{x})$  in (5)-(7) depend on the inverse fourth power of the ( $R_k$ ) to ( $R_{k+1}$ ) distances. Linearizing these terms (6)-(8) around a given trajectory will lead to severe errors even for small position errors, so this additional nonlinearity will further penalize robustness and stability weaknesses of control laws based on the linearized system. Amongst nonlinear approaches, differential flatness is widely used, yet  $\mathcal{S}_x$  is not generically linearizable by a dynamic feedback, so this approach can not apply to the generic case, as it is proven in section 4.4. Another idea is to apply a state feedback with a time-varying gain  $K(t)$  obtained by solving a differential Riccati equation; however solving the latter analytically is hardly possible. As in Olfati-Saber and Megretski (2001), a promising approach is to find how to map the system to normal feedback forms in order to propose backstepping controllers.

## 4 Main Results

The twofold contribution addresses first a controllability analysis for both the inertial microrobotic system  $\mathcal{S}_2^i$  and the non inertial system  $\mathcal{S}_m^{ni}$ , and then a control synthesis to Lyapunov stabilize these systems along any admissible reference trajectory.

### 4.1 System controllability

**Proposition 1** *System  $\mathcal{S}_2^i$  is strongly accessible and small-time controllable around  $\tilde{x} = 0$  if and only if both following conditions are satisfied:*

**C1** *Magnetic interaction exists:  $(i_1, j_1) \neq (0, 0)$ .*

**C2** The microrobots parameters  $(a_1, a_2, d_1, d_2, i_1, j_1)$  and the planned distance  $d_{1,2}(t)$  satisfy:

$$\frac{4(a_2 - a_1)^2(a_1 j_1 + a_2 i_1)}{a_1 a_2 d_{1,2}^5(t)} \neq (d_2 - d_1)(d_1 a_2 - d_2 a_1). \quad (9)$$

**Remark 1** Condition **C1** clearly requires –contrary to most previous studies– that the microrobots operate in close vicinity. Otherwise, there is no magnetic interaction, i.e.  $i_1 = j_1 = 0$ , leading to a noncontrollable linear system. In such a case, the system is simply stabilizable on a line depending on the initial condition  $\tilde{x}(0)$ . More precisely, both velocities are controllable as well as a linear combination of the microrobots positions: the system position is stabilized on a line  $\lambda \tilde{x}_1 + \mu \tilde{x}_2 = 0$  instead of the origin  $\tilde{x} = 0$ , with  $\lambda, \mu$  depending on  $\tilde{x}(0)$ , i.e. even point stabilization can not be achieved.

**Remark 2** The microrobots must have different designs as a consequence of condition **C2** since (9) is not satisfied if the microrobots are identical ( $d_1 = d_2$  and  $a_1 = a_2$ ), whatever  $d_{1,2}(t)$ . The resulting system is then not strongly accessible and consequently not controllable. If the two robots share the same magnetic sensitivity  $a$ , yet have different drag coefficients  $d_i$ , condition **C2** is fulfilled and the system is controllable for all  $d_{1,2}(t) \in \mathcal{D} \subset \mathbb{R} \setminus \{0\}$ .

When swimming at very low Reynolds  $Re \ll 1$ , the controllability result for an  $m$  non inertial microrobots underactuated system is given in the following proposition.

**Proposition 2** Consider  $(m - 1)$  identical microrobots  $(R_k)$ , so  $\epsilon_k = \varepsilon_k = \epsilon$  and  $\alpha_k = \alpha, \forall k \leq m - 1$ . Then system  $S_m^{ni}$  is small-time controllable around  $\tilde{x} = 0$  if and only if  $\epsilon_i, \varepsilon_i \neq 0$  and the last  $m$ -th robot  $(R_m)$  satisfies  $\alpha_m \neq \alpha$ .

**Remark 3** In the case of  $m = 3$  non inertial microrobots with no common parameter, the strong accessibility Lie rank condition  $\dim \Delta_{\mathfrak{C}_0}(\tilde{x}) = 3$  is fulfilled if and only if

$$\varpi \delta_1^{(1)} \delta_2^{(1)} \left( \delta_1^{(1)} \gamma_1 (\gamma_1 \varepsilon_1 + \gamma_2 (\varepsilon_1 + \epsilon_1)) - \delta_2^{(1)} \gamma_2 (\gamma_2 \varepsilon_2 + \gamma_1 (\varepsilon_2 + \epsilon_2)) \right) \neq 0 \quad (10)$$

where  $\gamma_k = \alpha_k - \alpha_{k+1}$ ,  $\varpi = \epsilon_1 \varepsilon_2 \alpha_2 + \varepsilon_1 \epsilon_2 \alpha_1 + \epsilon_1 \varepsilon_2 \alpha_3$  and  $\delta_k^{(1)}(\tilde{x}) = \frac{\partial \delta_k}{\partial \tilde{x}_k}(\tilde{x})$ . Considering one non magnetic microrobot ( $\epsilon_i = \varepsilon_i = 0$  for a given  $i$ ) hinders the system controllability so for an  $m = 3$  non inertial microrobotic system, **C1** is unchanged, while **C2** is replaced by (10). Of course, it is possible to satisfy (10) thanks to an appropriate choice of the distances  $d_k$ ; nonetheless, in the generic case considering  $m$  different microrobots, condition (10) last factor is a degree  $(m - 1)$  polynomial in  $\delta_k^{(1)}(\tilde{x})$  whose solving is not straightforward. That is the reason why Proposition 2 focuses on a simpler design consistent with standardized microrobots construction processes.

**Remark 4** If the drag force is nonlinear e. g. because of non-Newtonian effects, the proposed approach can still be used considering a first order Taylor expansion approximation of the drag force, i. e. linearization along the reference trajectory. Since the partially linearized system is controllable, then the nonlinear system is locally controllable.

#### 4.2 Proof of Proposition 1

If **C1** is not satisfied, nonlinear terms are removed from (5) so  $\dot{\tilde{x}} = A\tilde{x} + B\tilde{u}$ , and controllability is checked using the Kalman rank condition. Let  $\Gamma = (B \ AB \ \dots \ A^3 B)$ . Then  $\text{rank}(\Gamma) = 3 < 4$ , so system  $S_2^i$  is not fully controllable: only three modes are controllable and one is not. In closed-loop, the system poles can be placed at 0,  $\lambda_1, \lambda_2, \lambda_3$ , so the system is simply stable and  $\dot{\tilde{x}} = A_{cl}\tilde{x}$ , with e.g. distinct eigenvalues.  $A_{cl}$  is thus diagonalizable: there exists  $T = (t_{ij})$  such that the diagonal matrix  $D = T^{-1}A_{cl}T$  first entry is null. Since  $A_{cl}$  first two lines are  $(0_2 \ I_2)$ , then  $t_{31} = t_{41} = 0$ . Besides, since  $T$  is invertible, it follows that  $t_{11}^2 + t_{21}^2 \neq 0$ . Let  $z = T^{-1}\tilde{x}$ , then  $\dot{z} = Dz$ . As a result, it is clear that  $\forall t \geq 0 \ z_1(t) = z_1(0)$  and  $\lim_{t \rightarrow \infty} (z_2 \ z_3 \ z_4)(t) = (0 \ 0 \ 0)$ . Since  $\tilde{x} = Tz$ , it is straightforward that  $\lim_{t \rightarrow \infty} \tilde{x}(t) = (t_{11} \ t_{21} \ 0 \ 0) z_1(0)$ .

The strong accessibility algebra  $\mathfrak{C}_0$  is the smallest algebra that contains the control vector fields and such that  $[f, \mathfrak{C}_0] \subset \mathfrak{C}_0$ , with  $[\cdot, \cdot]$  denoting the Lie bracket operator. Let  $\Delta_{\mathfrak{C}_0}(\tilde{x}) = \text{span}\{X(\tilde{x}) : X \in \mathfrak{C}_0\}$ , the strong accessibility Lie rank condition  $\dim \Delta_{\mathfrak{C}_0}(\tilde{x}) = n = 4$  is a controllability necessary condition Nijmeijer and van der Schaft (1990). Let  $\Delta_a = a_1 - a_2$  and  $\Delta_d = d_1 - d_2$ , computing the successive brackets using the adjoint notation yields

$$ad_{fg}^1 = \begin{pmatrix} a_1 \\ a_2 \\ -d_1 a_1 \\ -d_2 a_2 \end{pmatrix}, ad_{fg}^2 = \begin{pmatrix} -d_1 a_1 \\ -d_2 a_2 \\ d_1^2 a_1 + i_1 \delta_1^{(1)} \Delta_a \\ d_2^2 a_2 - j_1 \delta_1^{(1)} \Delta_a \end{pmatrix} \quad (11)$$

$$ad_{fg}^3 = \begin{pmatrix} d_1^2 a_1 + i_1 \delta_1^{(1)} \Delta_a \\ d_2^2 a_2 - j_1 \delta_1^{(1)} \Delta_a \\ i_1 \delta_1^{(1)} (a_2 (d_1 + d_2) - 2d_1 a_1) - d_1^3 a_1 \\ j_1 \delta_1^{(1)} (a_1 (d_1 + d_2) - 2d_2 a_2) - d_2^3 a_2 \end{pmatrix} \quad (12)$$

$$[ad_{fg}^1, ad_{fg}^2] = \begin{pmatrix} 0 & 0 & i_1 & -j_1 \end{pmatrix}^T \delta_1^{(2)} \Delta_a^2$$

$$[ad_{fg}^1, ad_{fg}^3] = \begin{pmatrix} -i_1 \Delta_a \\ j_1 \Delta_a \\ i_1 (2d_1 a_1 - (d_1 + d_2) a_2) \\ j_1 (2d_2 a_2 - (d_1 + d_2) a_1) \end{pmatrix} \delta_1^{(2)} \Delta_a$$

with  $\delta_1^{(i)} = \frac{\partial^i \delta_1}{\partial \tilde{x}_1^i}$ . First, using (5b) and successive brackets (11)-(12) and higher length brackets,  $\text{span}\{g, [ad_f^1 g, ad_f^2 g], ad_f^1 g, [ad_f^1 g, ad_f^3 g], \dots\}$  is not full rank only for  $\Delta_a = 0$ . Besides,  $\text{span}\{ad_f^i g\}_{i \in \mathbb{N}}$  has a rank loss only if condition **C2** is violated. So  $\dim \mathcal{L}(f, g) < 4$  when both distributions are singular, *i. e.* when  $\Delta_a = \Delta_d = 0$ , and the system is thus not accessible at 0, and consequently not controllable when the microrobots are identical.

Now, when **C2** is fulfilled, since  $\dim \text{span}\{ad_f^i g\}_{i \in \mathbb{N}} = 4$ , then the system is strongly accessible at 0. However, strong accessibility does not imply controllability for a drift system since bad brackets can be an obstruction to controllability if they are not neutralized (spanned) by good brackets of smaller length. Bad brackets are iterated Lie brackets containing an odd number  $n_f$  of  $f$  and an even number  $n_g$  of  $g$ , like  $f, ad_g^2 f, [ad_f^1 g, ad_f^2 g]$  and so on. The length of an iterated Lie bracket  $X$  is computed as  $L_X = \theta n_f + n_g$  for some  $\theta \in [0, 1]$ . In the present case,  $f(0) = 0$  and  $ad_g^2 f = 0$ , so these bad brackets are neutralized. The bad bracket  $[ad_f^1 g, ad_f^2 g]$  of length  $L_b = 3\theta + 2$  is neutralized by lower good brackets (the  $ad_f^i g$  of length  $L_g = i\theta + 1 < L_b$ ) as long as condition **C2** is fulfilled since in such a case  $\dim \text{span}\{ad_f^i g\}_{i \in \mathbb{N}} = 4$ . Longer bad brackets are also neutralized since these lower length good brackets  $ad_f^i g$  already span the full space.

The only case still to be clarified is controllability when **C2** is violated. In Kawski (1987) Kawski gives a new necessary condition for controllability: if  $[ad_f^1 g, ad_f^2 g]$  is not spanned by  $g, ad_f^1 g, \dots, [ad_f^k g, ad_f^3 g]$  for  $k \in \mathbb{N}$ , then the system is not small-time local controllable. It is not difficult to show using (5b) that  $ad_g^2 f = 0$  so  $[ad_f^k g, ad_f^3 g] = 0$  for all  $k$ . Yet  $\dim \text{span}\{ad_f^i g\}_{i \in \mathbb{N}} = 3$  when condition **C2** is violated, so  $[ad_f^1 g, ad_f^2 g] \notin \text{span}\{ad_f^i g\}_{i \in \mathbb{N}}$ . Consequently the system is small-time local controllable if and only if both conditions **C1** and **C2** are fulfilled.

#### 4.3 Proof of Proposition 2

First note that when  $\alpha_m = \alpha$ ,  $ad_f^i g = 0$  for  $i \geq 1$ : the only non null brackets in the Lie algebra  $\mathcal{L}(f, g)$  are  $f$  and  $g$  so its dimension is only  $2 < m$  and hence the system is not controllable from any point. Lengthy yet simple induction shows that computing successively the Lie brackets  $h^i(\tilde{x}) = ad_f^i g(\tilde{x})$  for  $i \leq m - 1$  using the vector fields (7), the following properties hold for  $i \geq 1$ :

**P1:**  $h_j^i(\tilde{x}) = 0, \forall j \leq m - i - 1$ ;

**P2:**  $h_m^i(\tilde{x}) = -\frac{\varepsilon_{m-1}}{\varepsilon_{m-1}} \sum_{j=1}^{m-1} h_j^i(\tilde{x})$  for any  $\tilde{x}$  provided that  $m \leq 3$  and at  $\tilde{x} = 0$  for any  $m$ ;

**P3:**  $h_{m-i}^i(\tilde{x}) = (-1)^{i+1} \varepsilon_{m-1} \varepsilon^{i-1} (\alpha - \alpha_m) \prod_{k=1}^i \delta_{m-k}^{(1)}(\tilde{x})$ .

The dimension of the resulting strong accessibility algebra is thus  $m$  as long as  $\det C = \det ad_f^0 g, \dots, ad_f^{m-1} g \neq 0$ . Using properties **P1-P2** and adding to the last row of  $C$  the sum of all other rows weighted by  $\frac{\varepsilon_{m-1}}{\varepsilon_{m-1}}$  yields:

$$\det C = \begin{vmatrix} \alpha & 0 & \dots & h_1^{m-1} \\ \vdots & \vdots & & \star \\ \alpha & 0 & h_{m-2}^2 & \star \\ \alpha & h_{m-1}^1 & \star & \star \\ s & 0 & \dots & 0 \end{vmatrix} \quad (13)$$

with  $s = \alpha_m + (m - 1)\alpha \frac{\varepsilon_{m-1}}{\varepsilon_{m-1}}$ . Using the Laplace expansion along the last row, it follows that  $\det C = (-1)^{m+1+\frac{(m-1)(m+2)}{2}} s \prod_{i=1}^{m-1} h_{m-i}^i$  so property **P3** yields

$$\det C = (\varepsilon_{m-1} \alpha_m + \varepsilon_{m-1} (m - 1)\alpha) (\alpha_m - \alpha)^{m-1} \varepsilon^{\frac{(m-1)(m+2)}{2}} \varepsilon_{m-1}^{m-2} \prod_{i=1}^{m-1} \delta_i^{(1)^i}. \quad (14)$$

Since  $\varepsilon_{m-1} \varepsilon_{m-1} \geq 0$  and the  $\delta_i^{(1)}(\tilde{x}), i \leq m - 1$ , do not cancel on  $\tilde{\mathcal{X}}_m$ , controllability thus requires a non null magnetic interaction, and also requires that  $\alpha_m \neq \alpha$ .

#### 4.4 Lyapunov stabilizing controller

The proposed approach consists in two parts: first diffeomorphisms mapping systems  $\mathcal{S}_2^i$  and  $\mathcal{S}_m^{ni}$  to normal forms  $\mathcal{S}_i$  are exhibited depending on the parametric values, so the control synthesis for these normal forms then provides a Lyapunov stabilizing controller for the original systems  $\mathcal{S}_2^i$  and  $\mathcal{S}_m^{ni}$  full state in any case. In the sequel,  $A$  denotes a matrix in prime form,  $F$  and  $G$  are vector fields whose only last component is not null, and  $\mathcal{L}_f^i h$  denotes the  $i$ -th Lie derivative of  $h$  along  $f$ .

**Lemma 1** *Let cases A, B and C denote the parametric sets  $(a_1 \neq a_2, d_1 = d_2)$ ,  $(a_1 = a_2, d_1 \neq d_2)$  and  $(a_1 \neq a_2 \text{ and } d_1 \neq d_2)$  of  $\mathcal{S}_2^i$ , respectively. Let  $j \in \{A, B, C\}$ ,  $i = 4$  for cases A and B,  $i = 3$  for case C and*

$$\begin{cases} h^A = h^C : \tilde{x} \mapsto a_2 \tilde{x}_1 - a_1 \tilde{x}_2 & (15a) \\ h^B : \tilde{x} \mapsto d_1 \tilde{x}_1 - d_2 \tilde{x}_2 + \tilde{x}_3 - \tilde{x}_4 & (15b) \\ z_k = \phi_k^j(\tilde{x}) = \mathcal{L}_f^{k-1} h^j(\tilde{x}), k \leq i & (15c) \\ \xi = \phi_4^C(\tilde{x}) = \tilde{x}_1 - \tilde{x}_2 & (15d) \end{cases}$$

On  $\tilde{\mathcal{X}}$ , under controllability conditions of Proposition 1, the diffeomorphisms  $\phi^A$  and  $\phi^B$  map (5) to a pure feedback form  $\mathcal{S}_1 : \dot{z} = Az + F(z) + G(z)\tilde{u}$  in cases A and B,

with  $i = 4$ . In the generic case C, the diffeomorphism  $\phi^C$  defined for  $i = 3$  maps (5) to

$$(\mathcal{S}_2) \begin{cases} \dot{z} = Az + F(z, \xi) + G\tilde{u} \\ \dot{\xi} = f_\xi(z, \xi) \end{cases} \quad (16)$$

Besides,  $\mathcal{S}_2$  is a minimum phase system with respect to the origin  $(z, \xi) = 0$  provided that

$$\frac{a_1 - a_2}{d_2 - d_1}(a_2 i_1 + a_1 j_1) > 0. \quad (17)$$

The Lemma proof is given in Appendix A.

**Remark 5** In the particular cases A and B of Lemma 1, the system is differentially flat with a flat output  $y = h(\tilde{x})$  in (15a) and (15b). However, the system is not generically flat since it requires that the distributions  $\Delta_0 = \text{span}\{g\}$  and  $\Delta_{i+1}(\tilde{x}) = \text{span}\{\Delta_i, [f, \Delta_i]\}(\tilde{x})$  are involutive, i.e. stable by Lie bracketing. Using the vector fields given by (5b) and their brackets (11)-(12), it is not difficult to show that  $\Delta_2(\tilde{x})$  is involutive only in cases A or B. It is possible to propose a control law synthesis –and even a trajectory planning– using differential flatness in either case, yet we would rather present a control synthesis encompassing all possible cases, i.e. A, B or C.

**Lemma 2** Provided that the controllability condition of Proposition 2 is satisfied, let  $\delta_k^{(i)}(\tilde{x}) = \frac{\partial^i \delta_k}{\partial \tilde{x}_k^i}(\tilde{x})$  and

$$\begin{cases} h(\tilde{x}) = -[(m-2)\epsilon_{m-1}\alpha + \epsilon_{m-1}\alpha_m]\tilde{x}_1 \\ \quad + \alpha\epsilon_{m-1}\sum_{i=2}^{m-1}\tilde{x}_i + \alpha\epsilon_{m-1}\tilde{x}_m \\ z_{i+1} = \mathcal{L}^i h(\tilde{x}), i = 0, \dots, m-1, \end{cases} \quad (18)$$

then system  $S_m^{ni}$  is mapped to a pure feedback form  $S_1$ :  $\dot{z} = Az + F(z) + G(z)\tilde{u}$  with  $A$  in prime form and  $F, G$  whose only non null entry is the last one with

$$\begin{aligned} G_m(z) &= \epsilon^{m-2}\epsilon_{m-1}[(m-1)\epsilon_{m-1}\alpha + \epsilon_{m-1}\alpha_m] \\ &(\alpha - \alpha_m) \prod_{i=1}^{m-1} \delta_i^{(1)} \neq 0, \forall \tilde{x} \in \tilde{\mathcal{X}}_m. \end{aligned} \quad (19)$$

The proof of this Lemma is deferred to Appendix B.

**Proposition 3** Let  $(x_r(t), u_r(t))$  denote any admissible  $\mathcal{C}^1$  trajectory and the associated reference control input for  $S_2^i$  or  $S_m^{ni}$ . Provided that assumptions of Propositions 1 and 2 are fulfilled for systems  $S_2^i$  and  $S_m^{ni}$ , respectively, the control law  $u = \kappa_i(z, \xi)$  given by

$$\kappa_i(z, \xi) = u_r(t) - G_i^{-1}(z) \left( F_i(z, \xi) + \sum_{j=1}^i c_{i+1}^j z_j \right) \quad (20)$$

ensures the semiglobal exponential stability of the origin for any initial bounded state  $\tilde{x}(0) \in \tilde{\mathcal{X}}_0$  where  $c_i^j$  are constants recursively defined for gains  $k_j > 0$  by:

$$\begin{cases} c_i^i = 1, c_{i+1}^1 = k_i c_i^1 + c_{i-1}^1, c_{i+1}^i = \sum_{j=1}^i k_j \\ c_{i+1}^j = k_i c_i^j + c_i^{j-1} + c_{i-1}^j, j \in [2, i-1] \end{cases} \quad (21)$$

with a connected set  $\tilde{\mathcal{X}}_0 \subset \tilde{\mathcal{X}}$  and  $i = 4$  for system  $S_2^i$  in cases A and B,  $i = 3$  for system  $S_2^i$  in case C, and  $\tilde{\mathcal{X}}_0 \subset \tilde{\mathcal{X}}_m$  and  $i = m$  for system  $S_m^{ni}$ , respectively.

#### 4.5 Proof of Proposition 3

For system  $S_2^i$ , the backstepping procedure is iterated from step 1 to step  $i = 4$  on system  $\mathcal{S}_1$  in cases A and B, and up to  $i = 3$  and using the minimum phase property proven in Lemma 1 for system  $\mathcal{S}_2$  in case C. For system  $S_m^{ni}$ , the procedure is iterated up to step  $i = m$ .

1. Differentiating a first candidate Lyapunov function  $V_1 = \frac{1}{2}z_1^2$  leads to  $\dot{V}_1 = z_1 z_2$ . Set  $\bar{z}_1 = z_1$  and  $\bar{z}_2 = z_2 + k_1 z_1 = \sum_{r=1}^2 c_2^r z_r$  with  $k_1 > 0$  results in  $\dot{V}_1 = -k_1 \bar{z}_1^2 + \bar{z}_1 \bar{z}_2$ , with  $c_2^1 = k_1, c_2^2 = 1$  from (21). The last term is counterbalanced at next step.
2. Let  $V_2 = V_1 + \frac{1}{2}\bar{z}_2^2$  denote a second candidate Lyapunov function. From  $\bar{z}_2$  definition and using the normal form of systems  $\dot{z} = Az + F(z) + G(z)\tilde{u}$ , it follows that  $\dot{z}_2 = z_3 + k_1 z_2$  so  $\dot{V}_2 = -k_1 \bar{z}_1^2 + \bar{z}_2(z_1 + k_1 z_2 + z_3)$ . Let  $k_2 > 0$  and set  $\bar{z}_3 = \sum_{r=1}^3 c_3^r z_r$  with  $c_3^r$  given by (21), then we obtain

$$\dot{V}_2 = -k_1 \bar{z}_1^2 - k_2 \bar{z}_2^2 + \bar{z}_2 \bar{z}_3 \quad (22)$$

- j. At step  $j \leq i-1$ , define  $V_j = V_{j-1} + \frac{1}{2}\bar{z}_j^2$ , where

$$\bar{z}_j = \sum_{r=1}^j c_j^r z_r \quad (23)$$

with  $c_j^r$  given by (21). From steps 1 to  $j-1$  we have

$$\dot{V}_{j-1} = -\sum_{r=1}^{j-1} k_r \bar{z}_r^2 + \bar{z}_{j-1} \bar{z}_j. \quad (24)$$

Since, using (21),  $\varsigma = \bar{z}_{j-1} + \dot{\bar{z}}_j + k_j \bar{z}_j$  simplifies as

$$\begin{aligned} \varsigma &= (c_{j-1}^1 + k_j c_j^1)z_1 + \sum_{r=2}^{j-1} (c_{j-1}^r + k_j c_j^r + c_j^{r-1})\bar{z}_{j-1}^r \\ &\quad + (k_j c_j^j + c_j^{j-1})z_j + c_j^j z_{j+1} = \bar{z}_{j+1}, \end{aligned} \quad (25)$$

then, (23), (24) and (25) yields

$$\begin{aligned}\dot{V}_j &= - \sum_{r=1}^j k_r \bar{z}_r^2 + \bar{z}_j(\bar{z}_{j-1} + \dot{\bar{z}}_j + k_j \bar{z}_j) \\ &= - \sum_{r=1}^j k_r \bar{z}_r^2 + \bar{z}_j \bar{z}_{j+1}.\end{aligned}$$

- i. At final step  $i$ , we have to discriminate between systems  $\mathcal{S}_m^{ni}$  and  $\mathcal{S}_2^i$  in special cases A and B on the one hand, and  $\mathcal{S}_2^i$  in the generic case C on the other hand.

In the former case,  $\dot{z}_i = F_i(z) + G_i(z)\tilde{u}$  with  $i \in \{4, m\}$  for system  $\mathcal{S}_2^i$  in special cases A and B, and for system  $\mathcal{S}_m^{ni}$ , respectively. Since  $\dot{\bar{z}}_i = \sum_{r=1}^{i-1} c_i^r z_{r+1} + F_i(z) + G_i(z)\tilde{u}$ , differentiating  $V_i = V_{i-1} + \frac{1}{2}\bar{z}_i^2$  leads to:

$$\begin{aligned}\dot{V}_i &= - \sum_{r=1}^{i-1} k_r \bar{z}_r^2 + \bar{z}_i(\bar{z}_{i-1} + \sum_{r=1}^{i-1} c_i^r z_{r+1} \\ &\quad + F_i(z) + G_i(z)\tilde{u}).\end{aligned}\quad (26)$$

Using (23) for both  $j = i-1$  and  $j = i$  in (26) yields

$$\begin{aligned}\dot{V}_i &= - \sum_{r=1}^{i-1} k_r \bar{z}_r^2 + \bar{z}_i \left( c_{i-1}^1 z_1 + \sum_{r=1}^{i-1} (c_{i-1}^r z_r - c_{i-1}^{r-1}) z_r + c_{i-1}^{i-1} z_i + F_i(z) + G_i(z)\tilde{u} \right).\end{aligned}\quad (27)$$

Then, since  $G_i$  given by either (A.3), (A.5) or (19) is a never vanishing function on  $\tilde{\mathcal{X}}_0$ , using (20) in (27) and (21) again thus results in:  $\dot{V}_i = \sum_{r=1}^i k_r \bar{z}_r^2$ . Hence we obtain the exponential stability of  $\bar{z}$  from  $\dot{V}_i$  being negative definite. Since  $z$  and  $\bar{z}$  are linearly related, and since (15)-(18) define diffeomorphisms, it follows that  $z = 0$  and hence  $\tilde{x} = 0$  are exponentially stable.

In the latter case,  $i = 3$  and the error system is diffeomorphic to  $\mathcal{S}_3$ . Thus, we have  $\dot{z}_3 = F_3(z, \xi) + G_3\tilde{u}$ , so that  $\bar{z}_3 = \sum_{r=1}^3 c_3^r z_r$  dynamics are  $\dot{\bar{z}}_3 = c_3^1 z_2 + c_3^2 z_3 + F_3(z, \xi) + G_3\tilde{u}$  and differentiating  $V_3 = V_2 + \frac{1}{2}\bar{z}_3^2$  with  $\dot{V}_2$  given by (22) leads to

$$\dot{V}_3 = \bar{z}_3(\bar{z}_2 + \sum_{r=1}^2 c_3^r z_{r+1} + F_3 + G_3\tilde{u}) - \sum_{r=1}^2 k_r \bar{z}_r^2.$$

Note that  $G_3$  given by (A.6) is a non null constant, so choosing the control law  $\tilde{u} = -G_3^{-1}(\sum_{r=1}^3 c_3^r z_r + F_3(z, \xi))$  with some positive gain  $k_3$  using (21) thus ensures:

$$\dot{V}_3(z) = -k_1 z_1^2 - k_2 \bar{z}_2^2 - k_3 \bar{z}_3^2.\quad (28)$$

In this generic case C for system  $\mathcal{S}_2^i$ , *i.e.* when  $d_1 \neq d_2$  and  $a_1 \neq a_2$ , the system state is  $(z, \xi)$ .

We have proved that the function  $\dot{V}_3(\bar{z})$  is negative semi-definite, hence the manifold  $\mathcal{Z} = \{(z, \xi) \in \mathbb{R}^3 \times \mathbb{R} : z = 0\}$  is exponentially stable. Along this set, the system evolves on the zero dynamics  $\dot{\xi} = f_\xi(0, \xi)$ . We have shown in Lemma 1 that the only zero dynamics stable equilibrium point was  $\xi_a^* = 0$ . Using (15d), it results in the asymptotic stability of  $\mathcal{S}_{\tilde{x}}$  around zero.

## 5 Simulation results

Table 1

Inertial Microrobots Parameters

| Parameter [unit]                               | Symbol    | Case A | Case B | Case C |
|--|-----------|--------|--------|--------|
| Robots radius [ $10^{-6}m$ ]                   | $r_1$     | 200    | 200    | 200    |
|  | $r_2$     | 200    | 80     | 100    |
| Ferromagnetic ratio                            | $\tau_1$  | 0.85   | 0.85   | 0.85   |
|  | $\tau_2$  | 0.025  | 0.15   | 0.1    |
| Wall effect ratio                              | $\beta_1$ | 0.724  | 0.724  | 0.724  |
|  | $\beta_2$ | 0.724  | 0.888  | 0.860  |
| Control parameter [ $A.m^2.s^{-2}$ ]           | $a_1$     | 212.72 | 212.72 | 212.72 |
|  | $a_2$     | 6.25   | 212.72 | 25.02  |
| Drag parameter [ $s^{-1}$ ]                    | $d_1$     | 158.2  | 158.2  | 158.2  |
|  | $d_2$     | 158.2  | 4569.7 | 532.7  |
| Interaction parameter [ $10^{-10}m^5.s^{-2}$ ] | $i_1$     | 1.84   | 0.706  | 0.920  |
|  | $j_1$     | 1.84   | 62.5   | 7.55   |

Table 2

Physiological values in an ovarian artery

| Parameter [unit]                            | Symbol   | Value               |
|---|----------|---------------------|
| Blood viscosity [ $Pa.s$ ]                  | $\eta$   | $7 \cdot 10^{-3}$   |
| Vessel radius [ $m$ ]                       | $R$      | $1.5 \cdot 10^{-3}$ |
| Mean blood velocity [ $m.s^{-1}$ ]          | $a_0$    | $-70 \cdot 10^{-3}$ |
| Amplitude of the blood pulse [ $m.s^{-1}$ ] | $a_1$    | $9 \cdot 10^{-3}$   |
| Pulse [ $rad.s^{-1}$ ]                      | $\omega$ | $2\pi$              |
| Phase of the blood pulse [ $rad$ ]          | $\phi$   | 0                   |

The effectiveness of the proposed approach is illustrated first on an inertial two-agent microrobotic system  $\mathcal{S}_2^i$ , considering the three different classes of designs A, B and C. The two inertial microrobots ( $R_1$ ) and ( $R_2$ ) parameters are given in Table 1. Then a non inertial microrobotic system control is considered, for 5 non inertial robots ( $R_k$ ), whose parameters are given in Table 3 for  $Re \ll 1$ . Magnetic material is the same for all robots with  $M = 1.72 \cdot 10^6 A.m^{-1}$ . Parameters are such that the inertial and non inertial systems  $\mathcal{S}_2^i$  and  $\mathcal{S}_5^{ni}$  are controllable according to Propositions 1 and 2, respectively.

The pulsatile blood velocity is modeled using the Womersley model Womersley (1955) which results in a truncated Fourier series approximation. To be consistent with the vessel radius and simplify the study but without loss of generality, a first-order truncated Fourier series is considered

$$v_f(t) = a_0 + a_1 \cos(\omega t + \phi)\quad (29)$$

Table 3

Non Inertial Microrobots Parameters,  $k \leq 4, j \leq 3$ 

| Parameter [unit]                           | Symbol                     | Value                    |
|--|----------------------------|--------------------------|
| Robots radius [m]                          | $(r_k, r_5)$               | $(2.5, 5) 10^{-6}$       |
| Ferromagnetic ratio                        | $(\tau_k, \tau_5)$         | $(0.1, 0.85)$            |
| Wall effect ratio                          | $(\beta_k, \beta_5)$       | $(0.86, 0.724)$          |
| Control parameter<br>[ $A.m^2.s^{-1}$ ]    | $(\alpha_k, \alpha_5)$     | $(0.041, 1.176) 10^{-3}$ |
| Interaction parameters<br>[ $m^5.s^{-1}$ ] | $(\epsilon_j, \epsilon_j)$ | $-(2.78, 2.78)10^{-22}$  |
|  | $(\epsilon_4, \epsilon_4)$ | $-(1.89, 79.46)10^{-20}$ |

Table 4

Physiological values in an eye arteriole

| Parameter [unit]                            | Symbol   | Value         |
|---|----------|---------------|
| Blood viscosity [ $Pa.s$ ]                  | $\eta$   | $5 10^{-3}$   |
| Vessel radius [m]                           | $R$      | $35 10^{-6}$  |
| Mean blood velocity [ $m.s^{-1}$ ]          | $a_0$    | $-2 10^{-3}$  |
| Amplitude of the blood pulse [ $m.s^{-1}$ ] | $a_1$    | $0.1 10^{-3}$ |
| Pulse [ $rad.s^{-1}$ ]                      | $\omega$ | $2\pi$        |
| Phase of the blood pulse [ $rad$ ]          | $\phi$   | $0$           |

with a negative mean value so that the microrobots have to swim against the flow. The physiological datas are given in Tables 2 and 4 for a small artery and an arteriole.

### 5.1 Inertial Microrobots $S_2^i$

In the following simulations, the Reynolds number lies in the range  $[0; 2.5]$  so inertial effects can not be neglected. The microrobot ( $R_1$ ) is the same in the three simulations, whilst the parameters of the second microrobot are modified in each simulation (see Table 1) so as to illustrate the two special cases A and B, and lastly the generic case C. Initial condition is given by

$$x_0 = \begin{pmatrix} 0.005 & -0.0025 & 0 & 0 \end{pmatrix}^T \in \mathcal{X}^+. \quad (30)$$

The admissible reference trajectories are computed using Fruchard et al. (2020) for the same given desired distance  $d_{1,2}$ . With parameters from Table 1, initial conditions on  $x_r(t)$  are given in Table 5.

Table 5

Inertial Microrobots: Planning &amp; Control Parameters

| Parameter              | Symbol    | Case A  | Case B  | Case C  |
|------------------------|-----------|---|---|---|
| Control gains          | $k_1$     | 40  | 10  | 300   |
|                        | $k_2$     | 5   | 850   | 5   |
|                        | $k_3$     | 20  | 400   | 1   |
|                        | $k_4$     | 5   | 10  | —   |
| Reference distance [m] | $d_{1,2}$ | $2 10^{-3}$   | $2 10^{-3}$   | $2 10^{-3}$   |
| Reference state        | $x_{r0}$  | $\begin{pmatrix} 0 \\ -0.002 \\ 0 \\ 0 \end{pmatrix}$ | $\begin{pmatrix} 0 \\ -0.002 \\ 0.014 \\ 0.014 \end{pmatrix}$ | $\begin{pmatrix} 0 \\ -0.002 \\ 0 \\ 0 \end{pmatrix}$ |

#### 5.1.1 First simulation Case A

In this configuration, the microrobots have the same radius and density, and are consequently equally affected by the drag force since  $d_1 = d_2$ . However, the first one has a high ferromagnetic ratio contrary to the second one which is mainly composed of a therapeutic load.

Figure 2a illustrates the convergence of both positions and velocities of the two microrobots to their references after a 2 s long transient phase. During this phase, the control effort is high to bring the system along the admissible reference. The ( $R_1$ ) to ( $R_2$ ) distance, initially set to 7.5 mm, quickly reduces to 1.4 mm before stabilizing at the desired distance  $d_{1,2}$ . The nonlinear magnetic interaction term  $\delta_1(\tilde{x})$  depends on that distance and severely impacts the system dynamics. To overcome the magnetic interaction which increases as the robots get closer down to 1.4 mm, the control input depicted on Figure 2c has an overshoot during the first 0.1 s though not reaching saturation. The system error depicted on Figure 2b is then stabilized to zero. The control input is depicted in Figure 2c: saturation is not reached and the input tends to  $0.114 T.m^{-1}$ . To follow the same trajectory, had the first microrobot been alone, it would have required only a fifth of the control effort (around  $0.025 T.m^{-1}$ ); but if the second microrobot had been alone, the control input would have reached  $0.835 T.m^{-1}$ , *i.e.* far beyond the actuator limitations, because of its very poor ferromagnetic ratio. The present simulation thus illustrates the interest in using the first robot to tow the second one by taking advantage of the interaction magnetic force to relax the control effort.

#### 5.1.2 Second simulation Case B

In the special case B, the microrobots share the same magnetic sensitivity  $a$  to the control input but have not the same drag coefficient since the second microrobot is far smaller than the first one.

The control input reaches both the upper and lower saturations for  $t \leq 0.04$  s, as can be noticed on Figure 2f. Saturation events do not impact severely the tracking and the control effort is far smaller than in case A over this period. However, contrary to the previous simulation, the robots distance does not go below 1.6 mm so the interaction force remains small, what explains why the control effort in case B is smaller than in case A considering the first 0.2 s, despite the initial saturations. After a 1 s long transient phase, Figure 2e shows that the error is stabilized to zero.

#### 5.1.3 Third simulation Case C

This simulation illustrates the generic situation where the microrobots have no common parameter  $d$  nor  $a$ . Table 1 shows that microrobot ( $R_2$ ) is chosen so as to satisfy condition (17) of Lemma 1, *e.g.* having less magnetic material and a higher drag parameter than the first

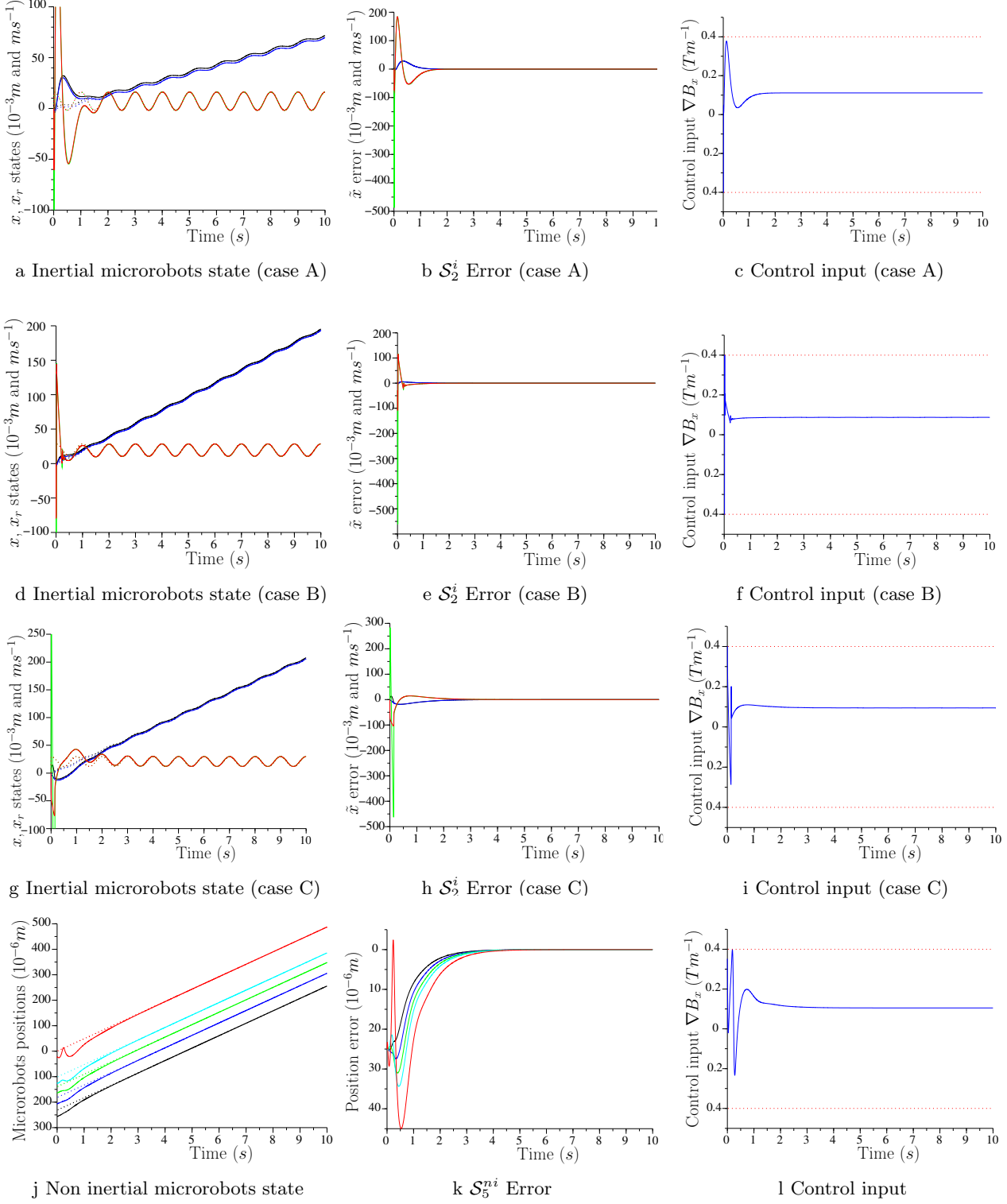


Fig. 2. From top to bottom: simulations for two inertial microrobots  $\mathcal{S}_2^i$  in cases A, B and C, and simulation for 5 non inertial microrobots  $\mathcal{S}_5^{ni}$ . (a), (d), (g): Microrobots ( $R_1$ ) and ( $R_2$ ) positions ( $x_1, x_2$ ) and velocities ( $x_3, x_4$ ) are depicted in black, blue, green and red solid lines, their reference trajectories are depicted in dashed lines; (j): Microrobots positions (solid lines) and reference trajectories (dotted lines) for robots ( $R_1$ ), ( $R_2$ ), ( $R_3$ ), ( $R_4$ ) and ( $R_5$ ) are depicted in black, blue, green, cyan and red lines, respectively. (b), (e), (h): State of the error system  $\mathcal{S}_2^i$ ; (k): State of the error system  $\mathcal{S}_5^{ni}$ . (c), (f), (i), (l): the single control input of the systems with saturations  $\pm 0.4 T.m^{-1}$  depicted in red dash-dotted lines.

robot, so that the error system is a minimum phase system with respect to the origin.

The simulation is quite similar to the previous one, except that the saturation occurs only at  $t = 0$  s (see Figure 2i). The control input stabilizes the set  $\mathcal{Z} = \{(z, \xi) \in \mathbb{R}^3 \times \mathbb{R} : z = 0\}$  within 3 seconds and the internal state  $\xi = \tilde{x}_1 - \tilde{x}_2$  is stabilized due to the minimum phase property. The distance between the two microrobots is given by  $\xi + d_{1,2}$ . Since  $\xi$  is not directly controlled, this distance grows quickly to 20 mm thus inducing a far reduced magnetic interaction between the robots, before it converges to the desired  $d_{1,2} = 2$  mm value, as depicted in Figure 2g.

## 5.2 Non Inertial Microrobots $\mathcal{S}_5^{ni}$

Table 6  
Non Inertial Microrobots: Planning & Control Parameters

| Parameter               | Symbol      | Value                                    |
|-------------------------|-------------|--|
| Control gains           | $k$         | $(5 \ 6 \ 15 \ 19 \ 4)^T$                |
| Reference distances [m] | $d_{i,i+1}$ | $-(50 \ 42 \ 38 \ 101.6)^T 10^{-6}$      |
| Reference state [m]     | $x_{r0}$    | $-(231.6 \ 130 \ 92 \ 50 \ 0)^T 10^{-6}$ |

In arterioles, the radius and the relative velocity of the microrobots in the blood are smaller (see Table 4, resulting in a Reynolds number  $Re \approx 2 \cdot 10^{-3} \ll 1$  for the biggest microrobot ( $R_5$ ) and twice smaller for ( $R_k$ ),  $k \leq 4$ ). The microrobots inertia can be neglected and the 5-agent system is well modeled by a non inertial system  $\mathcal{S}_5^{ni}$ . We consider a 5-agent system where the leader ( $R_5$ ) is highly magnetized as can be noticed in Table 3. Thus, thanks to the attractive magnetic interaction, ( $R_5$ ) tows the four smaller and mainly payload filled identical microrobots ( $R_k$ ),  $k \leq 4$ , along a pre-planned trajectory computed using reference distances  $d_{k,k+1}$  and initial state  $x_{r0}$  given in Table 6. The control input is computed using Lemma 2 and Proposition 3 with gains of Table 6. The system state  $x_0$  is initialized at  $(x_{r0} - 25 \cdot 10^{-6}) m \in \mathcal{X}_m^-$ .

Since the initial error is important and because of the underactuation constraints on the system, the microrobots have to manoeuvre to reach the planned trajectory as depicted in Figure 2j. During the transient phase, Figure 2k shows that the ( $R_5$ ) position error  $\tilde{x}_5$  peaks up to nearly 4  $\mu m$  despite a strictly decreasing Lyapunov function. Indeed, the choice of a small gain  $k_5$  makes it possible to use mainly the leader as a degree of freedom to manoeuvre the followers: ( $R_5$ ) is highly attractive for ( $R_4$ ) so this attraction dominates the system dynamics. Besides, since ( $R_5$ ) contains more magnetic material, it is more sensitive to the magnetic actuation than other robots and the strategy is here to stabilize  $\tilde{x}_5$  after all other states have converged. During the first 0.2 s, ( $R_4$ ) is highly attracted by ( $R_5$ ), so error  $\tilde{x}_4$  decreases, which in turn attracts ( $R_3$ ) along the reference trajectory. Then, due to the increasing distance between ( $R_5$ )

and ( $R_4$ ), the resulting magnetic interaction on ( $R_4$ ) becomes negative til 0.4 s, so ( $R_4$ ) is attracted by ( $R_3$ ) whilst the control input changes sign to bring back ( $R_5$ ) closer to the other robots. Figure 2l illustrates the control input: on the very beginning,  $u < 0$  which may seem counter-intuitive since  $\tilde{x}_k < 0$ , yet since ( $R_5$ ) is the more reactive robot it reduces the distance between ( $R_5$ ) and ( $R_4$ ) while not affecting too much other robots, thus inducing a strong attraction on ( $R_4$ ) to recover the planned trajectory. The next manoeuvre is clearly visible during the interval [0.2; 0.4] s when  $u$  sign changes to bring back ( $R_5$ ) after peaking. After 1 s, there is no more manoeuvre and the tracking convergence looks like the tracking of a fully actuated system. Finally,  $u$  converges to  $u_r \approx 0.1 T m^{-1}$  where the control input mainly compensates for the pulsatile blood flow. It is worth mentioning that controlling a single microrobot of type ( $R_k$ ),  $k \leq 4$ , along the same trajectory would have required a 300 bigger control effort (more than  $29 T m^{-1}$ ) than used here to control five microrobots simultaneously.

## 6 Discussion and conclusion

The present paper has presented a controllability analysis and a novel approach to synthesize control laws aiming at Lyapunov stabilizing the trajectory of magnetic microrobots navigating in a blood vessel using the same single control input. To this end, a sufficient and necessary controllability condition is given for this nonlinear underactuated system with drift, which was lacking in the existing literature. In particular, microrobots have to both operate in close vicinity and be designed carefully. A unified Lyapunov stabilizing control law has then been proposed, with concerns about the possible configurations of the microrobotic system. This control synthesis relies on a two steps method: the system is first proven to be diffeomorphic to different nonlinear canonical forms, and a backstepping synthesis coupled with a zero dynamics stability analysis is proposed. Simulations have highlighted the interest in using the magnetic interaction so that one of the microrobots can pull or push the other ones, thus reducing the control efforts required to propel the latter.

Further perspectives, which are currently under investigation, are threefold. First, since therapeutic goals may require that the system has to follow a non admissible trajectory, it would be interesting to analyze under what conditions –at least practical– stabilization can be ensured. Another key point for the control of multiple magnetic microrobots, which has not yet been addressed in the nonlinear case except in Sun et al. (2019), is the synthesis of observers in order to propose stabilizing output feedbacks. Lastly, biophysical systems are unlikely to be free from parametric and modeling errors. For instance, in the present paper, the blood velocity is supposed known whilst it is likely that this information is hardly

accessible to measurement, thus implying errors in its amplitude, number of harmonics, or frequency. Ongoing work is thus led to ensure stability despite these uncertainties, an issue that we have already addressed for a single microrobot using either adaptive approach Arcese et al. (2013) or state estimation in Sadelli et al. (2017). Our recently developed low-power high gain observer for fluid mechanics application Ahmed et al. (2020) is also promising for estimation of the blood flow despite an unknown blood pulse and inherent possible observability defects.

## Acknowledgements

The author is grateful to the Editor and anonymous reviewers for their insightful and helpful suggestions to improve the quality of this work.

## A Proof of Lemma 1

Under conditions **C1** and **C2**, it has been shown from (5b), (11)-(12) that  $\dim \text{span}_{i=0..3} \{ad_f^i g\}(0) = 4$ . Now let us seek for a function  $h$  whose differential is a basis of the annihilator of  $\Delta = \text{span}_{i=0..2} \{ad_f^i g\}(\tilde{x})$ :

$$dh \left( g \quad ad_f g \quad ad_f^2 g \right) (\tilde{x}) = 0. \quad (\text{A.1})$$

If such a function can be exhibited, then choosing  $z_{i+1} = \mathcal{L}_f^i h(\tilde{x})$  maps  $\mathcal{S}_2^i$  to the pure feedback form  $\mathcal{S}_1$ . Let  $h_i = \frac{\partial h}{\partial \tilde{x}_i}(\tilde{x})$ , (A.1) first equation leads to:

$$a_1 h_3 + a_2 h_4 = 0, \quad (\text{A.2})$$

that is  $h(\tilde{x}_1, \tilde{x}_2, a_2 \tilde{x}_3 - a_1 \tilde{x}_4)$ . Solving the last two equations of (A.1) will depend on the system parameters.

- 1 If  $d_1 = d_2$ , *i. e.* in case A, using (A.2), the second equation of (A.1) gives  $a_1 h_1 + a_2 h_2 = 0$ , and using (A.2) in the third equation of (A.1) leads to  $h_3 = 0$ . One then deduces that  $h$  depends only on  $(a_2 \tilde{x}_1 - a_1 \tilde{x}_2)$ . Besides, the choice (15a) yields  $\left| \frac{\partial z}{\partial \tilde{x}} \right| = -(a_1 - a_2)^2 (a_2 i_1 + a_1 j_1) \delta_1^{(1)^2}(\tilde{x}) \neq 0$  since  $\delta_1^{(1)}$  is a non-vanishing function on any compact. (15a)-(15c) thus defines a diffeomorphism mapping  $\mathcal{S}_2^i$  on  $\mathcal{S}_1$ . Note that, in this particular case, the system controllability is ensured only if  $a_1 \neq a_2$  so as to satisfy condition **C1**. A straightforward differentiation yields:

$$F_4(z) = -d_1 z_4 - ((d_1(\tilde{x}_4 - \tilde{x}_3) - (i_1 + j_1)\delta_1)\delta_1^{(1)} + (\tilde{x}_3 - \tilde{x}_4)^2 \delta_1^{(2)})(a_2 i_1 + a_1 j_1) \quad (\text{A.3})$$

$$G_4(z) = -(a_2 i_1 + a_1 j_1)(a_1 - a_2)\delta_1^{(1)}.$$

- 2 If  $d_1 \neq d_2$ , using (A.2), (A.1) second equation yields  $a_1 h_1 + a_2 h_2 - a_1(d_1 - d_2)h_3 = 0$  which, combined with (A.2) in (A.1) last equation gives:

$$\begin{aligned} & \left( -a_1 d_1 + a_1(d_1 + d_2) + \gamma \frac{\delta_1^{(1)}(\tilde{x})}{a_2} \right) h_1 \\ &= - \left( -a_2 d_2 + a_2(d_1 + d_2) + \gamma \frac{\delta_1^{(1)}(\tilde{x})}{a_1} \right) h_2 \end{aligned} \quad (\text{A.4})$$

with  $\gamma = \frac{(a_1 - a_2)(a_2 i_1 + a_1 j_1)}{(d_1 - d_2)}$ . Now let solve the partial differential equations inherited from (A.4):

$$\frac{\partial h}{\partial \tilde{x}_1} = a_2 d_1 + \gamma \frac{\delta_1^{(1)}(\tilde{x})}{a_1}, \quad \frac{\partial h}{\partial \tilde{x}_2} = -a_1 d_2 - \gamma \frac{\delta_1^{(1)}(\tilde{x})}{a_2}.$$

It is not difficult to show, *e.g.* by a proof by contradiction, that  $dh$  is an exact differential form if and only if  $a_1 = a_2 = a$  since it leads to  $\gamma = 0$ . So, for case B, one infers that  $h$  is given by (15b). Let  $\iota = i_1 + j_1$ , since  $\left| \frac{\partial z}{\partial \tilde{x}} \right| = -(d_2 - d_1)^2 (i_1 + j_1)^3 \delta_1^{(1)^3}(\tilde{x}) \neq 0$ , the diffeomorphism (15b)-(15c) maps  $\mathcal{S}_2^i$  to the feedback normal form  $\mathcal{S}_1$  with:

$$\begin{aligned} F_4(z) &= -\iota [d_1^2 \tilde{x}_3 - d_2^2 \tilde{x}_4 - (d_1 i_1 + d_2 j_1) \delta_1] \delta_1^{(1)} \\ &\quad + \iota (\tilde{x}_3 - \tilde{x}_4) \left( 3(d_2 \tilde{x}_4 - d_1 \tilde{x}_3 - \iota \delta_1) \delta_1^{(2)} \right. \\ &\quad \left. (\tilde{x}_3 - \tilde{x}_4)^2 \delta_1^{(3)} + \iota \delta_1^{(1)^2} \right) \end{aligned} \quad (\text{A.5})$$

$$G_4(z) = -\iota a (d_2 - d_1) \delta_1^{(1)}.$$

- 3 In the generic case C,  $d_1 \neq d_2$  and  $a_1 \neq a_2$ . In the light of the foregoing analysis, there exists no transformation mapping  $\mathcal{S}_2^i$  into the pure feedback form. However, the choice of  $h$  as in (15a) yields by differentiation to  $\mathcal{S}_2$  with:

$$\begin{aligned} F_3(z, \xi) &= d_1^2 a_1 \tilde{x}_3 - d_2^2 a_2 \tilde{x}_4 + \nu \delta_1 \\ &\quad - (a_2 i_1 + a_1 j_1) (\tilde{x}_3 - \tilde{x}_4) \delta_1^{(1)} \end{aligned} \quad (\text{A.6})$$

$$G_3 = a_1 a_2 (d_2 - d_1)$$

$$f_\xi(z, \xi) = \frac{(a_1 d_2 - a_2 d_1) z_2 + \Delta_a (z_3 + (a_2 i_1 + a_1 j_1) \delta(\xi))}{a_1 a_2 (d_2 - d_1)}$$

where  $\Delta_a = a_1 - a_2$  and  $\nu = d_1 a_2 i_1 + d_2 a_1 j_1$ . Since  $\left| \frac{\partial z, \xi}{\partial \tilde{x}} \right| = a_1 a_2 (a_1 - a_2) (d_2 - d_1) \neq 0$  from (15d), then (15a) and (15c)-(15d) define a global diffeomorphism.

Now let us study the zero dynamics of the system  $\mathcal{S}_2$ , *i.e.*  $\dot{\xi} = f_\xi(0, \xi)$ . From (15a)-(15d), it is clear that:

$$\begin{cases} z_1 = a_2 \tilde{x}_1 - a_1 \tilde{x}_2, & z_2 = a_2 \tilde{x}_3 - a_1 \tilde{x}_3 \\ z_3 = -d_1 a_2 \tilde{x}_3 + d_2 a_1 \tilde{x}_4 - (a_2 i_1 + a_1 j_1) \delta_1(\tilde{x}). \end{cases} \quad (\text{A.7})$$

Recall that  $\delta_1 : \xi \mapsto \frac{1}{(\xi + d_{1,2}(t))^4} - \frac{1}{d_{1,2}^4(t)}$  and set

$z = 0$ , it follows from (A.6)-(A.7) that:

$$f_\xi(0, \xi) = \frac{(a_1 - a_2)(a_2 i_1 + a_1 j_1)}{a_1 a_2 (d_2 - d_1)} \left( \frac{1}{(\xi + d_{1,2})^4} - \frac{1}{d_{1,2}^4} \right).$$

The equilibrium points of the zero dynamics are thus given by  $\xi_a^* = 0$  and  $\xi_b^* = -2d_{1,2}$ . Linearizing the last equation of  $\mathcal{S}_2$  along  $z = 0, \xi = \xi^*$  gives:

$$\dot{\xi} = -\frac{4(a_1 - a_2)(a_2 i_1 + a_1 j_1)}{a_1 a_2 (\xi^* + d_{1,2}(t))^5 (d_2 - d_1)} \xi, \quad (\text{A.8})$$

so that the equilibrium points  $\xi_a^*$  and  $\xi_b^*$  are respectively asymptotically stable and unstable provided that (17) is satisfied. So  $\mathcal{S}_2$  is a minimum phase system with respect to the equilibrium point  $(z, \xi) = 0$  under the aforementioned condition.

## B Proof of Lemma 2

If the assumptions of Proposition 2 are fulfilled, system  $\mathcal{S}_m^{ni}$  is small-time controllable. As in the previous proof, to simplify the control synthesis, a diffeomorphism mapping system  $\mathcal{S}_m^{ni}$  to a pure feedback form is sought. Searching for a function  $h$  whose differential is a basis of  $\Delta = \text{span}_{i=0..m-2} \{ad_f^i g\}$  annihilator leads to  $(m-1)$  relationships using the first  $(m-1)$  columns of (13). Let  $h_i$  denote the partial differential of  $h$  with respect to  $\tilde{x}_i$ . Due to the triangular form of the  $ad_f^i g(\tilde{x})$ , one proceeds recursively as follows:

- Using the second relationship  $dh \ ad_f g(\tilde{x}) = 0$  that involves only  $h_{m-1}$  and  $h_m$ , since  $(\alpha - \alpha_m)\delta_{m-1}^{(1)}(\tilde{x}) \neq 0$  on  $\tilde{\mathcal{X}}_m$ , one gets a first integral  $w_1(\tilde{x}) = \tilde{x}_{m-1} + \frac{\epsilon_{m-1}}{\epsilon_m} \tilde{x}_m$ . So  $h$  is invariant on the foliation  $w_1$  being constant.
- Let  $h_{w_1} = \frac{\partial h}{\partial w_1}$ . Since  $dh \ ad_f^2 g(\tilde{x}) = 0$  involves only  $h_{m-2}$  and  $h_{w_1}$ , and  $\delta_{m-2}^{(1)}(\tilde{x}) \neq 0$  on  $\tilde{\mathcal{X}}_m$ , another first integral is given by  $w_2(\tilde{x}) = \tilde{x}_{m-2} + w_1$  so  $h(\tilde{x}_1, \dots, \tilde{x}_{m-3}, w_2)$ .
- At step  $i < m$ ,  $i$ -th equation  $dh \ ad_f^i g(\tilde{x}) = 0$  depends only on  $h_{m+1-i}$  and  $h_{w_{i-2}}$  where  $w_j(\tilde{x}) = \tilde{x}_{m-j} + w_{j-1}, \forall j \leq i-2$ . Hence one deduces from  $\delta_{m+1-i}^{(1)}(\tilde{x}) \neq 0$  that  $h(\tilde{x}_1, \dots, \tilde{x}_{m-i}, w_{i-2})$ .
- Lastly, using the first relationship  $dh \ ad_f^0 g(\tilde{x}) = 0$  and the fact that  $\delta_1^{(1)}(\tilde{x})$  never cancels on  $\tilde{\mathcal{X}}_m$ , it follows that  $h$  depends only on  $w_{m-1}(\tilde{x}) = -((m-2)\alpha\epsilon_{m-1} + \alpha_m\epsilon_{m-1})\tilde{x}_1 + \alpha\epsilon_{m-1}w_{m-2}$ .

Consequently, defining  $h$  and  $z$  as in (18) results in a pure feedback system  $\mathcal{S}_1$  with  $F_m = \mathcal{L}_f^m h(\tilde{x})$ . The mapping  $\psi : \tilde{x} \rightarrow z$  is characterized by a jacobian matrix whose determinant is computed adding all columns in the second one, then factorizing on line  $2 \leq j \leq m-1$  by

$\epsilon^{j-1}((m-1)\epsilon_{m-1}\alpha + \epsilon_{m-1}\alpha_m)$  and performing a Laplace expansion along the second column to get a lower triangular matrix. The Jacobian is then easily computed as:

$$\left| \frac{\partial \psi(\tilde{x})}{\partial \tilde{x}} \right| = (-1)^m (\alpha_m - \alpha) \varrho_m \prod_{i=1}^{m-1} \delta_i^{(1) m-i},$$

$$\varrho_m = ((m-1)\epsilon_{m-1}\alpha + \epsilon_{m-1}\alpha_m)^{m-1} \epsilon^{\frac{(m+1)(m-2)}{2}} \epsilon_{m-1}^2.$$

By controllability assumption in Proposition 2,  $\varrho_m \neq 0$ , and since the partial derivatives  $\delta_i^{(1)}$  do not cancel on  $\tilde{\mathcal{X}}_m$ ,  $\psi$  is a diffeomorphism. For the same reasons, it follows that  $G_m$ , obtained by induction as (19), is non null on  $\tilde{\mathcal{X}}_m$ , and hence can be inverted.

## References

- M. C. Lagomarsino, F. Capuani, and C. P. Lowe. A simulation study of the dynamics of a driven filament in an aristotelian fluid. *Journal of Theoretical Biology*, 224(2):215–224, 2003.
- A. A. Evans and E. Lauga. Propulsion by passive filaments and active flagella near boundaries. *Physical Review E*, 82(4):041915.1–041915.12, 2010.
- R. Dreyfus, J. Beaudry, M. L. Roper, M. Fermigier, H. A. Stone, and J. Bibette. Microscopic artificial swimmers. *Nature*, 437:862–865, 2005.
- L. Zhang, K. E. Peyer, and B. J. Nelson. Artificial bacterial flagella for micromanipulation. *Lab on a chip*, 10(17):2203–2215, 2010.
- J. J. Abbott, K. E. Peyer, M. C. Lagomarsino, L. Zhang, L. X. Dong, I. K. Kaliakatsos, and B. J. Nelson. How should microrobots swim? *International Journal of Robotics Research*, 28:1434–1447, 2009.
- J.-B. Mathieu, G. Beaudoin, and S. Martel. Method of propulsion of a ferromagnetic core in the cardiovascular system through magnetic gradients generated by an MRI system. *IEEE Transactions on Biomedical Engineering*, 53(2):292–299, 2006.
- B. J. Nelson, I. K. Kaliakatsos, and J. J. Abbott. Microrobots for minimally invasive medicine. *Annual Review of Biomedical Engineering*, 12:55–85, 2010.
- L. Giralaldi and J. B. Pomet. Local controllability of the two-link magneto-elastic micro-swimmer. *IEEE Transactions on Automatic Control*, 62(5):2512–2518, 2017.
- M. Fruchard, L. Arcese, and E. Courtial. Estimation of the blood velocity for nanorobotics. *IEEE Transactions on Robotics*, 30(1):93–102, 2014.
- B. R. Donald, C. G. Levey, and I. Paprotny. Planar microassembly by parallel actuation of MEMS microrobots. *Journal of Microelectromechanical Systems*, 17(4):789–808, 2008.
- S. Floyd, C. Pawashe, and M. Sitti. Two-dimensional contact and noncontact micromanipulation in liquid using an untethered mobile magnetic microrobot. *IEEE Transactions on Robotics*, 25(6):303–308, 2009.

- D.R. Frutiger, B.E. Kratochvil, K. Vollmers, and B.J. Nelson. Small, fast, and under control: wireless resonant magnetic micro-agents. *International Journal of Robotics Research*, 29(5):613–636, 2010.
- A. Servant, F. Qiu, M. Mazza, K. Kostarelos, and B. J. Nelson. Controlled in vivo swimming of a swarm of bacteria-like microrobotic flagella. *Advanced Materials*, 27(19):2981–2988, 2015.
- S. Martel and M. Mohammadi. Using a swarm of self-propelled natural microrobots in the form of flagellated bacteria to perform complex micro-assembly tasks. In *IEEE International Conference on Robotics and Automation*, pages 500–505, May 2010.
- P. Vartholomeos, M. R. Akhavan-Sharif, and P. E. Dupont. Motion planning for multiple millimeter-scale magnetic capsules in a fluid environment. *IEEE International Conference on Robotics and Automation*, pages 1927–1932, May 2012.
- S. Floyd, E. Diller, C. Pawashe, and M. Sitti. Control methodologies for a heterogeneous group of untethered magnetic micro-robots. *International Journal of Robotics Research*, 30(13):1553–1565, 2011.
- E. Diller, S. Floyd, C. Pawashe, and M. Sitti. Control of multiple heterogeneous magnetic microrobots in two dimensions on nonspecialized surfaces. *IEEE Transactions on Robotics*, 28(1):172–182, 2012.
- M. Salehizadeh and E. Diller. Two-agent formation control of magnetic microrobots in two dimensions. *Journal of Micro-Bio Robotics*, 12(1):9–19, 2017.
- A. Eqtami, O. Felfoul, and P. E. Dupont. MRI-powered closed-loop control for multiple magnetic capsules. *IEEE International Conference on Intelligent Robots and Systems*, pages 3536–3542, September 2014.
- Mohammad Salehizadeh and Eric D. Diller. Path planning and tracking for an underactuated two-microrobot system. *IEEE Robotics and Automation Letters*, 6(2):2674–2681, 2021.
- M. Fruchard, L. Sadelli, and A. Ferreira. Local controllability, trajectory planning, and stabilization of a two-agent underactuated microrobotic system. *IEEE Systems Journal*, 14(2):2892–2900, 2020.
- L. Arcese, M. Fruchard, and A. Ferreira. Endovascular magnetically-guided robots: navigation modeling and optimization. *IEEE Transactions on Biomedical Engineering*, 59(4):977–987, 2012.
- L. Arcese, M. Fruchard, and A. Ferreira. Adaptive controller and observer for a magnetic microrobot. *IEEE Transactions on Robotics*, 29(4):1060–1067, 2013.
- W. L. Haberman and R. M. Sayre. *Motion of Rigid and Fluid Spheres in Stationary and Moving Liquids Inside Cylindrical Tubes*. David Taylor Model Basin Report 1143. Department of the Navy, Hydromechanics Laboratory, 1958.
- P. Vartholomeos and C. Mavroidis. In silico studies of magnetic microparticle aggregations in fluid environments for MRI-guided drug delivery. *IEEE Transactions on Biomedical Engineering*, 59(11):3028–3038, 2012.
- E. M. Purcell. Life at low reynolds number. *American Journal of Physics*, 45:3–11, 1977.
- A. N. Tikhonov. Systems of differential equations containing small parameters in the derivatives. *Matematicheskii Sbornik*, 73(3):575–586, 1952.
- S. Tamaz, R. Gourdeau, A. Chanu, J-B. Mathieu, and S. Martel. Real-time MRI-based control of a ferromagnetic core for endovascular navigation. *IEEE Transactions on Biomedical Engineering*, 55(7):1854–1863, 2008.
- M. Mehrtash and M. B. Khamesee. Design and implementation of LQG/LTR controller for a magnetic tele-manipulation system-performance evaluation and energy saving. *Microsystem Technology*, 17(5-7):1135–1143, 2011.
- J. Choi, S. Jeong, K. Cha, L. Qin, J. Li, J. Park, S. Park, and B. Kim. Position stabilization of microrobot using pressure signal in pulsating flow of blood vessel. In *IEEE Sensors*, pages 723–726, November 2010.
- R. Olfati-Saber and A. Megretski. *Nonlinear Control of Underactuated Mechanical Systems with Application to Robotics and Aerospace Vehicles*. PhD thesis, USA, 2001.
- H. Nijmeijer and A. van der Schaft. *Nonlinear Dynamical Control Systems*. Springer-Verlag, Berlin, Heidelberg, 1990. ISBN 0-387-97234-X.
- M. Kawski. A necessary condition for local controllability. *Contemporary Mathematics*, 68:143–155, 1987.
- J. R. Womersley. Method for the calculation of velocity, rate of flow and viscous drag in arteries when the pressure gradient is known. *The Journal of physiology*, 127(3):553–563, 1955.
- Y. Sun, M. Fruchard, and A. Ferreira. Output feedback synthesis for a two-agent nonlinear microrobotic system. In *58th IEEE Conference on Decision and Control, CDC*, pages 6844–6850, December 2019.
- L. Sadelli, M. Fruchard, and A. Ferreira. 2D observer-based control of a vascular microrobot. *IEEE Transactions on Automatic Control*, 62(5):2194–2206, 2017.
- J. Ahmed, M. Fruchard, E. Courtial, and Y. Touré. Low-power high gain observers for wake flow rebuild. In *59th IEEE Conference on Decision and Control, CDC*, pages 5428–5434, December 2020.



**Matthieu Fruchard** received the Dipl. Ing. and M.S. degrees from the Ecole Centrale of Lille - University of Lille, France, in 2001, and the Ph.D. degree in control theory from the Ecole des Mines de Paris, Sophia-Antipolis, France, in 2005. He joined the laboratory PRISME (Laboratoire Pluridisciplinaire de Recherche en Ingénierie des Systèmes, Mécanique et Energétique), University of Orléans, France, in 2007, where he currently is Associate Professor, and head of the Control Theory team since 2018. His research interests include control and observer synthesis for classes of nonlinear systems using Lyapunov theory, with applications especially to microrobotics and fluid mechanics.